EVOLUTION OF DERIVATIVE SINGULARITIES IN HYPERBOLIC QUASILINEAR SYSTEMS OF CONSERVATION LAWS

Evolution of derivative singularities in hyperbolic quasilinear systems of conservation laws

R. Arnold[1], R. Camassa[1], G. Falqui[2,4,5], G. Ortenzi[2,4], M. Pedroni[3,4]

[1] *University of North Carolina at Chapel Hill, Carolina Center for Interdisciplinary Applied Mathematics, Department of Mathematics, Chapel Hill, NC 27599, USA*
rvincent@live.unc.edu, camassa@amath.unc.edu

[2] *Department of Mathematics and Applications, University of Milano-Bicocca, Via Roberto Cozzi 55, I-20125 Milano, Italy*
gregorio.falqui@unimib.it, giovanni.ortenzi@unimib.it

[3] *Dipartimento di Ingegneria Gestionale, dell'Informazione e della Produzione, Università di Bergamo, Viale Marconi 5, I-24044 Dalmine (BG), Italy*
marco.pedroni@unibg.it

[4] *INFN, Sezione di Milano-Bicocca, Piazza della Scienza 3, 20126 Milano, Italy*

[5] *SISSA, via Bonomea 265, 34136 Trieste, Italy*

Abstract

Motivated by problems arising in the piecewise construction of physically relevant solutions to models of shallow water fluid flows, we study the initial value problem for quasilinear hyperbolic systems of conservation laws in $1+1$ dimensions when the initial data are continuous with "corners," i.e., derivative discontinuities. While it is well known that generically such discontinuities propagate along characteristics, under which conditions the initial corner points may fission into several ones, and which characteristics they end up following during their time evolution, seems to be less understood; this study aims at filling this knowledge gap. To this end, a distributional approach to moving singularities is constructed, and criteria for selecting the corner-propagating characteristics are identified. The extreme case of initial corners occurring with at least a one-sided infinite derivative is special. Generically, these gradient catastrophe initial conditions for hyperbolic systems (or their parabolic limits) can be expected to evolve instantaneously into either shock discontinuities or rarefaction waves. It is shown that when genuine nonlinearity does not hold uniformly and fails at such singular points, solution continuity along with their infinite derivative persist for finite times. All the results are demonstrated in the context of explicit solutions of problems emerging from applications to fluid flows.

1 Introduction

Models of water wave propagation, both surface and internal to a density stratified fluid, often lead to a "core" hyperbolic structure (see eg., [17, 15, 4] for a partial list), and in this context self-similar special exact solutions provide useful information on the evolution of more general initial data [2, 3]. In order to be physically relevant, these special solutions must be spliced between constant states, leading to discontinuous derivatives, whose evolution can in principle be tracked within the model

thanks to general tools for hyperbolic systems. In fact, as is well known, a hyperbolic system of partial differential equations (see e.g. [17]) admits solutions with persisting discontinuous derivatives of some order along characteristics, e.g., corners when considering discontinuous first derivatives. However, no reference to the initial value problem under such circumstances appears to have received much attention in the literature on the subject, to the best of our knowledge. In fact, the issue of how such corners evolve from those possibly present at the initial time can be somewhat subtle: in systems with more than one dependent variable, corners in the initial data may have to "fission" or split into several ones following multiple families of characteristics. The precise way in which splitting of corners and other singularities occur in physically relevant models is the subject of this work.

Specifically, we consider (i) the splitting of corner points and (ii) solutions containing points where the spatial derivative is infinite but the solution evolves continuously without smoothing or the formation of a jump discontinuity for a quasilinear hyperbolic system of conservation laws. For the splitting of corners, an approach using a distributional ansatz is developed, further elaborating an idea from [3], which led to a conjecture [2] formulated in terms of Riemann invariants. This distributional approach allows us to extend the conjecture to the more generic case, in higher dimensions, where Riemann invariants may not exist, and further to generalize the classical approach (as described in, e.g., [17]) to the emergence of several corners from a single point. Then it is shown how the failure of genuine nonlinearity (see below for a definition) is necessary and sufficient for the sustenance of an infinite spatial derivative along a characteristic without evolution to either of the most typical scenarios, i.e., instantaneous smoothing or shock formation. In fact, unlike these familiar scenarios, both (i) and (ii) are cases that do not seem to have received sufficient attention in the literature. Finally, in the second half of the paper, these results are discussed in relation to explicit solutions of systems arising in shallow water flow. We find that the splitting of corners seen in [2, 3] is generic, thus our examples will focus on the less common non-splitting of corners.

This paper is organized as follows. Relevant notation is introduced in section 2. In sections 3 and 4, the respective general problems of splitting of corners points and persistent infinite gradients are addressed. Section 5 is dedicated to examples of applications arising in the study of dynamics of shallow water fluid flows.

2 Notation

Let $\boldsymbol{U}(x,t)$ be the mapping of (a subset of) the space-time half-plane $(x,t) \in \mathbb{R} \times \mathbb{R}^+$ to an n-dimensional vector in $\mathbb{R}^n$, i.e., $\boldsymbol{U} : \mathbb{R} \times \mathbb{R}^+ \to \mathbb{R}^n$, defined to be the solution of the quasilinear system

$$\partial_t \boldsymbol{U} + \partial_x\big(\boldsymbol{F}(\boldsymbol{U})\big) = 0. \tag{2.1}$$

The Jacobian matrix $D\boldsymbol{F}$ with components $A_{ij} \equiv \partial F_i/\partial U_j$ where dropping bolds and adding subscripts indicates taking vector components, is assumed diagonalizable with real and distinct eigenvalues $\lambda_1(\boldsymbol{U}) < \lambda_2(\boldsymbol{U}) < ... < \lambda_n(\boldsymbol{U})$. We denote a corresponding set of right eigenvectors by $\boldsymbol{r}_1, \boldsymbol{r}_2, ..., \boldsymbol{r}_n$. For our purposes the function $\boldsymbol{F} : \mathbb{R}^n \to \mathbb{R}^n$ is assumed to be at least twice continuously differentiable. Henceforth, we will not use Einstein convention of summation over repeated indices, and sums will always be explicitly indicated.

For completeness, we recall here elements of distributional calculus and how an equation such as (2.1) can be cast in weak form in order to define solutions with a lower degree of regularity than the equation as stated demands, not requiring a solution be smooth, continuous or even a function at all. The solutions thus allowed are defined as follows. If K is the space of infinitely differentiable and compactly supported functions on a given domain Ω (test functions), in our case $\Omega = \mathbb{R} \times \mathbb{R}^+ \to \mathbb{R}^n$,

then a continuous linear functional $\Lambda : K \to \mathbb{R}$ is known as a generalized function (see, e.g., [7]), and can be differentiated according to the rules

$$\partial_x \Lambda(\phi) \equiv -\Lambda(\partial_x \phi),$$

and

$$\partial_t \Lambda(\phi) \equiv -\Lambda(\partial_t \phi),$$

for all test functions $\phi \in K$. If f is any function, measurable on Ω, a functional Λ_f can be defined by

$$\Lambda_f(\phi) \equiv \int_\Omega f(x,t)\phi(x,t)dxdt.$$

When a generalized function Λ_f appears in this way, we abuse notation by identifying it with f.

Assuming only that $\boldsymbol{U}$ is a generalized function and using this definition, equation 2.1 becomes

$$\int_0^\infty \int_{-\infty}^\infty \left((\partial_t \phi)\boldsymbol{U} + (\partial_x \phi)\big(\boldsymbol{F}(\boldsymbol{U})\big)\right) dxdt + \int_{-\infty}^\infty \boldsymbol{U}(x,0)\phi(x,0)dx = 0, \tag{2.2}$$

for any test function ϕ, with initial condition

$$\boldsymbol{U}(x,0) = \boldsymbol{U}_0(x). \tag{2.3}$$

Our usage of generalized functions will be restricted to (see below)

$$J_m(x) \equiv \frac{x^m}{m!} H(x) \tag{2.4}$$

where $H(x)$ is the Heaviside function. The identity

$$J_m'(x) = \partial_x J_m(x) = J_{m-1}(x) \tag{2.5}$$

is easily obtained. With these differential identities in mind, it will be possible to bypass the direct use of (2.2) and continue to use (2.1) even when $\boldsymbol{U}$ is not continuously differentiable. Note that in order for derivatives to be carried over to test functions, it is required that (2.1) is in conservation form (though, for the non-conservative case, other methods can be devised to handle weak solutions, as in reference [17]).

A common assumption known as genuine nonlinearity (see [9, 10]) is

$$D\lambda_k(\boldsymbol{U}) \cdot \boldsymbol{r}_k \neq 0. \tag{2.6}$$

In the present work we shall consider the failure of this condition, i.e., the existence of points $\boldsymbol{U}$ where

$$D\lambda_k(\boldsymbol{U}) \cdot \boldsymbol{r}_k = 0, \tag{2.7}$$

in multiple settings (see also e.g. [13, 14, 16, 6, 12, 11] for further applications, in particular to the problem of shocks). We shall call the manifold of such points the NGNL (for "non-genuinely-nonlinear") manifold.

3 Splitting of corner points

In this section we consider how a gradient jump in an initial condition for a hyperbolic system (2.2) will split, traveling on a subset of the characteristics emanating from the point $(x,t) = (x_0, 0)$, where $\boldsymbol{U}_0(x)$ is continuously differentiable except at $x = x_0$:

$$\lim_{x \to x_0^-} (\boldsymbol{U}_0)_x \neq \lim_{x \to x_0^+} (\boldsymbol{U}_0)_x \,, \tag{3.1}$$

where from here on we will use subscripts to denote derivatives with respect to the independent variables. In this section we assume both derivatives exist and are finite (infinite derivatives are treated in section 4). This occurs when at least one of the components of $\boldsymbol{U}_0$ has a discontinuous first derivative at a given point. We shall derive criteria for the presence of such a corner on a given characteristic (assuming Lipschitz continuity of certain coefficients whose form is determined by the flux function $\boldsymbol{F}$). In this context a conjecture from reference [2] is proven, namely that corners split off their initial conditions exactly along the characteristics for which there are corners in the corresponding Riemann invariants, when these can be found.

Let $x = \chi_k(t; x_0)$ with $\chi_k(0; x_0) = x_0$ be a curve on which a derivative jump moves (these will usually but not always be characteristics; at a parabolic degeneracy for instance, as occurs at vacuum points [2], a complete set of characteristics does not exist. See remark 3 below for further discussion of this case), labeled by some indices $\{k\}$ arranged so that

$$\chi_j(t; x_0)|_{t=0} \leq \chi_k(t; x_0)|_{t=0},$$

when $j < k$. Then we define

$$\lim_{x \to \chi_k(t;x_0)^-} \boldsymbol{U}_x(x,t) \equiv (\boldsymbol{U}_x^l)_k(t), \tag{3.2}$$

$$\lim_{x \to \chi_k(t;x_0)^+} \boldsymbol{U}_x(x,t) \equiv (\boldsymbol{U}_x^r)_k(t), \tag{3.3}$$

and we denote derivative jump by square brackets,

$$[\boldsymbol{U}_x]_k(t) \equiv (\boldsymbol{U}_x^r)_k(t) - (\boldsymbol{U}_x^l)_k(t). \tag{3.4}$$

Similarly, jump quantities are defined for the flux function $\boldsymbol{F}$, namely

$$\lim_{x \to \chi_k(t;x_0)^-} \boldsymbol{F}(\boldsymbol{U})_x(x,t) \equiv (\boldsymbol{F}_x^l)_k(t), \tag{3.5}$$

$$\lim_{x \to \chi_k(t;x_0)^+} \boldsymbol{F}(\boldsymbol{U})_x(x,t) \equiv (\boldsymbol{F}_x^r)_k(t), \tag{3.6}$$

$$[\boldsymbol{F}_x]_k(t) \equiv (\boldsymbol{F}_x^r)_k(t) - (\boldsymbol{F}_x^l)_k(t). \tag{3.7}$$

Further, we define $(\boldsymbol{U}_{xx}^l)_k$, $(\boldsymbol{U}_{xx}^r)_k$, $(\boldsymbol{F}_{xx}^l)_k$, $(\boldsymbol{F}_{xx}^r)_k$, $[\boldsymbol{U}_{xx}]_k$ and $[\boldsymbol{F}_{xx}]_k$ analogously. In order to isolate the derivative jumps from the otherwise smooth evolution we write, with the above notation

$$\boldsymbol{U}(x,t) = \tilde{\boldsymbol{U}}(x,t) + \sum_j \Big([\boldsymbol{U}_x]_j(t) J_1(x - \chi_j(t;x_0)) + [\boldsymbol{U}_{xx}]_j(t) J_2(x - \chi_j(t;x_0)) \Big) \tag{3.8}$$

and

$$\boldsymbol{F}(x,t) = \tilde{\boldsymbol{F}}(x,t) + \sum_j \Big([\boldsymbol{F}_x]_j(t) J_1(x - \chi_j(t;x_0)) + [\boldsymbol{F}_{xx}]_j(t) J_2(x - \chi_j(t;x_0)) \Big) \tag{3.9}$$

where $\tilde{\boldsymbol{U}}(x,t)$ is twice differentiable.

We have made no explicit assumptions about the index set $\{j\}$, but it usually consists of a subset of the n characteristic families. We will return to this below, pointing out some intriguing exceptional cases which we leave to future work.

Using equations (3.8), (3.9) and (2.5) in (2.2), we obtain the vanishing condition

$$0 = \sum_j \Big((-\chi_j' [\boldsymbol{U}_x]_j + [\boldsymbol{F}_x]_j) J_0(x-\chi_j) + (-\chi_j' [\boldsymbol{U}_{xx}]_j + [\boldsymbol{F}_{xx}]_j + [\boldsymbol{U}_x]_j') J_1(x-\chi_j) \Big) + \psi(x,t) \quad (3.10)$$

where the zero on left hand side is the zero distribution, primes denote differentiation with respect to time, $\psi(x,t)$ stands for the remainder obtained by lumping together the tilded fields and the J_2 terms, and is hence once continuously differentiable with respect to x. For any given index $j=k$ both the coefficients of the one-sided functions J_0 and J_1 must vanish in the limit $x \to \chi_k$. The vanishing of the J_0 coefficient as $x \to \chi_k(t)$, may be written

$$0 = -\chi_k' [\boldsymbol{U}_x]_k + [D\boldsymbol{F}\, U_x]_k = (-\chi_k' I + D\boldsymbol{F})[\boldsymbol{U}_x]_k \quad (3.11)$$

for $t>0$, where I denotes the $n \times n$ identity matrix, and we have used the the regularity assumptions on the flux function $\boldsymbol{F}$ (we emphasize that χ_k' factors out of jump expressions since it is the same on both sides of $x=\chi_k$). Formula (3.11) is, of course, the characteristic equation for k-th characteristic velocity $\lambda_k = \chi_k'$, so that $[\boldsymbol{U}_x]_k$ is proportional to the corresponding eigenvector,

$$[\boldsymbol{U}_x]_k = c_k \boldsymbol{r}_k, \quad (3.12)$$

with c_k the proportionality factor. However, if we take the limit as $t \to 0$, the expansion is still valid at $t=0$, allowing us to analyze the possible splitting of any individual corner present in the initial data and further to avoid relying on Taylor expansions (as in [17]) which do not apply to the splitting case from initial data.

The vanishing condition for the J_1 coefficient in (3.10), once again making use of the assumed regularity of $\boldsymbol{F}$, is then

$$\begin{aligned} 0 &= -\lambda_k [\boldsymbol{U}_{xx}]_k + \big(D\boldsymbol{F}[\boldsymbol{U}_{xx}]_k + [D^2\boldsymbol{F}(\boldsymbol{U}_x, \boldsymbol{U}_x)]_k \big) + [\boldsymbol{U}_x]_k' \\ &= (D\boldsymbol{F} - \lambda_k I)[\boldsymbol{U}_{xx}]_k + D^2\boldsymbol{F}([\boldsymbol{U}_x]_k, [\boldsymbol{U}_x]_k) + 2D^2\boldsymbol{F}((\boldsymbol{U}_x^l)_k, [\boldsymbol{U}_x]) + [\boldsymbol{U}_x]_k' \\ &= (D\boldsymbol{F} - \lambda_k I)[\boldsymbol{U}_{xx}]_k + c_k^2 D^2\boldsymbol{F}(\boldsymbol{r}_k, \boldsymbol{r}_k) + c_k \Big(2D^2\boldsymbol{F}((\boldsymbol{U}_x^l)_k, \boldsymbol{r}_k) + D\boldsymbol{r}_k (D\boldsymbol{F})(\boldsymbol{U}_x^l)_k \Big) + c_k' \boldsymbol{r}_k. \end{aligned} \quad (3.13)$$

Multiplying by the suitably normalized left eigenvector $\boldsymbol{l}_k$ yields (cf. [17])

$$0 = c_k' + c_k \boldsymbol{l}_k \cdot (D\boldsymbol{r}_k (D\boldsymbol{F})(\boldsymbol{U}_x^l)_k + 2D^2\boldsymbol{F}((\boldsymbol{U}_x^l)_k, \boldsymbol{r}_k)) + c_k^2\, \boldsymbol{l}_k \cdot D^2\boldsymbol{F}(\boldsymbol{r}_k, \boldsymbol{r}_k). \quad (3.14)$$

For the proportionality factor c_k this is a homogeneous (non-autonomous, nonlinear) ordinary differential equation (ODE) which, if its coefficients are Lipschitz continuous, will have a unique solution given an initial condition $c_k(0) = c_k^0$. Thus, if $c_k^0 = 0$ no corners can develop, and, conversely, we see that a corner will propagate along precisely the characteristics for which

$$c_k^0 = \boldsymbol{l}_k(\boldsymbol{U}_0(x_0)) \cdot [(\boldsymbol{U}_0)_x] \neq 0. \quad (3.15)$$

For the case when Riemann invariants exist, denoted here by $R^j(\boldsymbol{U})$, we recall that they must satisfy the constraints (see e.g., [17]) that their differential is a left-eigenvector of DF, that is

$$DR^j = \beta_j \boldsymbol{l}_j, \quad (3.16)$$

for some proportionality factors β_j. Hence, for the case when jumps are present along the k-th characteristic and Riemann invariants exist,

$$\begin{aligned}[R_x^j]_k &= DR^j \cdot [\boldsymbol{U}_x]_k \\ &= \beta_j \boldsymbol{l}_j \cdot (c_k \boldsymbol{r}_k) \\ &= \delta_{jk}\beta_j c_k. \end{aligned} \tag{3.17}$$

From this relation, a few consequences for this case when Riemann invariants exist can be derived. First, (3.17) shows that a derivative discontinuity will propagate along the k-th characteristic when the corresponding k-th Riemann invariant has a corner in its initial condition. Conversely, when $\beta_k(\boldsymbol{U}_0(x_0)) \neq 0$, i.e., $\boldsymbol{U}_0(x_0)$ is not a critical point for the given Riemann invariant, if the initial k-th Riemann invariants does not have a corner then the coefficients c_k must vanish, $c_k = 0$, and hence no corner will develop for the dependent variable $\boldsymbol{U}(x,t)$ along the corresponding characteristic. Further, corners for the dependent variables $\boldsymbol{U}(x,t)$ may coexist with C^1-continuity (i.e., no derivative jump) for the corresponding Riemann invariants, provided these have critical points at the corner values of $\boldsymbol{U}$. An example of this will be given in section 5.3 below.

Several remarks concerning the general case are now in order:

Remark 1. Our approach above extends the one used in [17] by using distributions, which allows simultaneous consideration of multiple characteristics, and hence the possible splitting of corners from a single initial one.

Remark 2. The non-conservative case

$$\boldsymbol{U}_t + A(\boldsymbol{U})\boldsymbol{U}_x = 0 \tag{3.18}$$

does not immediately fit in the above approach which stems from (2.2); however, an expansion consistent with the conservative case may be obtained by taking a one sided Taylor expansion of the entire equation and requiring the various order coefficients to vanish, as was done in [17].

Remark 3. The form of expansion in the above remark can be applied to shock formation at a point of parabolic degeneracy. This occurs in particular for vacuum points in the Airy shallow water system (see (5.1)) at what is known as the "physical vacuum singularity" (see [2]).[1] In this case the vanishing of the J_0 coefficient in (3.10), i.e., the characteristic equation, may not be satisfiable when the k-family has a non-trival Jordan block at $\boldsymbol{U}_0(x_0)$. In particular, if $[\boldsymbol{U}_x]_k$ is a generalized eigenvector then

$$(D\boldsymbol{F} - \lambda_k I)[\boldsymbol{U}_x]_k \neq 0. \tag{3.19}$$

This can be remedied, however, by adding $[\boldsymbol{U}]_k J_0(x-\chi_k)$ and $[\boldsymbol{F}]_k J_0(x-\chi_k)$ terms to the respective expansions (3.8) and (3.9) (terms which we assume to vanish at initial time as we still wish to consider continuous initial conditions). Then the vanishing condition for the coefficient of $J_0(x-\chi_k)$ becomes

$$[\boldsymbol{U}]_k' = (D\boldsymbol{F} - \lambda_k I)[\boldsymbol{U}_x]_k, \tag{3.20}$$

producing a jump for any $t > 0$, even though the initial conditions do not suffer a gradient catastrophe.

Remark 4. In the particular case of the Airy system, the formation of shocks in this way at the vacuum only appears when the velocity is regarded as being defined at the vacuum by Rankine-Hugoniot conditions for the conservation. These conditions happen be to compatible with the physically correct Rankine-Hugoniot conditions for the conservation of momentum (see [2]).

[1] See [5] for a similar approach to the appearance of δ-shocks.

4 Persistent infinite derivatives in continuous solutions

In this section we focus on a special case in the solutions of system (2.1), whereby a point at which a vertical gradient occurs, and persists without evolving into either a shock or a finite slope. Specifically, we show that a persistent vertical gradient in a continuous solution may only occur at points where genuine nonlinearity fails. Let $\chi(t)$ be a curve along which an infinite gradient persists in a continuous solution $\boldsymbol{U}$ in a hyperbolic system. We do not assume from the outset that $\chi(t)$ is a characteristic since infinite derivatives could be associated with shocks which do not move along characteristics. The spatial derivative may be decomposed in terms of the right eigenvectors:

$$\boldsymbol{U}_x = \sum_k \alpha_k(x,t)\boldsymbol{r}_k(\boldsymbol{U}(x,t)). \tag{4.1}$$

Choosing $\boldsymbol{r}_k$ to be bounded, of unit magnitude say, a vertical gradient is present exactly when

$$\lim_{x\to\chi(t)^-} \alpha_j(x,t) = \pm\infty \tag{4.2}$$

for at least one index j where we have assumed without loss of generality that the blowup occurs in the left limit $x \to \chi(t)^-$. Differentiating $\boldsymbol{U}$ along the curve $x = \chi(t)$ gives

$$\frac{d}{dt}\boldsymbol{U}(\chi(t),t) = \sum_k \alpha_k(\chi(t),t)\{\chi'(t) - \lambda_k(\boldsymbol{U}(\chi(t),t))\}\boldsymbol{r}_k(\boldsymbol{U}(\chi(t),t)) \tag{4.3}$$

and, assuming the solution has bounded variation along this curve, the derivative cannot blowup identically so $\chi'(t) = \lambda_j$ for a unique j, i.e., $\chi(t)$ is a characteristic (if we only require a continuous solution to exist on one side of the curve, then $\chi(t)$ could be an envelope of characteristics). Thus we write

$$\chi(t) = \chi_j(t; x_0) \tag{4.4}$$

where $x_0 = \chi(0)$ and

$$\lim_{x\to\chi_j(t;x_0)^-} \alpha_j(x,t) = \pm\infty. \tag{4.5}$$

To show that a persistent vertical gradient in a continuous solution may only occur at points where genuine nonlinearity fails, we shall proceed by contradiction. In fact, suppose that genuine nonlinearity holds at a persistent infinite gradient of (one of) the components of the solution $\boldsymbol{U}$, and $(\lambda_j)_x$ is bounded along $x = \chi(t)$. The spatial derivative of λ_j is given by

$$(\lambda_j)_x = D\lambda_j \cdot \boldsymbol{U}_x = \sum_k \alpha_k D\lambda_j \cdot \boldsymbol{r}_k \tag{4.6}$$

so that the sum is dominated by the α_j term going to $\pm\infty$ (note that this is not so when genuine nonlinearity fails on $x = \chi(t)$, in which case the whole expression may still be bounded). Without loss of generality we can assume that $\alpha_j \to +\infty$ (otherwise we may replace $\boldsymbol{U}(x,t)$ with $\boldsymbol{U}(-x,-t)$ and work backwards in time) and, using the genuine nonlinearity assumption, choose $\boldsymbol{r}_j$ so that

$$D\lambda_j \cdot \boldsymbol{r}_j > 0. \tag{4.7}$$

In this case

$$\lim_{x\to\chi(t)} (\lambda_j)_x(x,t) = \infty\,, \qquad \text{i.e.,} \quad \lim_{x\to\chi(t)} \frac{1}{(\lambda_j)_x(x,t)} = 0^+ \tag{4.8}$$

for all t (at least on some time interval $[0, T)$). Then using (4.4), we have for any $\epsilon > 0$ and $x_2 < x_1 < x_0$ there exists $\delta > 0$ such that the inequalities

$$|x_1 - x_0|, |x_2 - x_0| < \delta$$

imply that

$$\epsilon > \frac{\chi_j(t; x_1) - \chi_j(t; x_2)}{\lambda_j(\chi_j(t; x_1), t) - \lambda_j(\chi_j(t; x_2), t)}. \tag{4.9}$$

For conciseness of notation, we replace the explicit dependence on x_α, $\alpha = \{1, 2\}$, with a superscript α in the functions χ_j (and hence λ_j) above. Then we may rewrite (4.9) as

$$\begin{aligned}
\epsilon &> \frac{\chi_j^1(t) - \chi_j^2(t)}{\lambda_j^1(t) - \lambda_j^2(t)} \\
&= \frac{x_1 - x_2 + \int_0^t \lambda_j^1(\tau) - \lambda_j^2(\tau) d\tau}{\lambda_j^1(t) - \lambda_j^2(t)} \\
&= \frac{x_1 - x_2}{\chi_j^1(t) - \chi_j^2(t)} \frac{\chi_j^1(t) - \chi_j^2(t)}{\lambda_j^1(t) - \lambda_j^2(t)} + \int_0^t \frac{\lambda_j^1(\tau) - \lambda_j^2(\tau)}{\lambda_j^1(t) - \lambda_j^2(t)} d\tau \\
&= \frac{x_1 - x_2}{\chi_j^1(t) - \chi_j^2(t)} \frac{1}{(\lambda_j)_x(x_*(t), t)} + \int_0^t \frac{\lambda_j^1(\tau) - \lambda_j^2(\tau)}{\lambda_j^1(t) - \lambda_j^2(t)} d\tau
\end{aligned} \tag{4.10}$$

for some $\chi_j^2(t) < x_*(t) < \chi_j^1(t)$, by the mean value theorem. The integral on the right approaches a multiple of t as $t \to 0$, i.e., if we fix t, it can be bounded below by $b\,t$ for any $0 < b < 1$ by taking the parameter interval of t to be sufficiently small. Thus if we fix some $b > 0$ and correspondingly restrict the parameter interval of t, we have

$$\frac{x_1 - x_2}{\chi_j^1(t) - \chi_j^2(t)} \frac{1}{(\lambda_j)_x(x_*(t), t)} + \int_0^t \frac{\lambda_j^1(\tau) - \lambda_j^2(\tau)}{\lambda_j^1(t) - \lambda_j^2(t)} d\tau \geq \int_0^t \frac{\lambda_j^1(\tau) - \lambda_j^2(\tau)}{\lambda_j^1(t) - \lambda_j^2(t)} d\tau > bt \tag{4.11}$$

which contradicts relation 4.10 since this is supposed to hold for any $\epsilon > 0$. We have thus arrived at a contradiction by assuming that an infinite gradient may persist in a continuous solution when genuine nonlinearity holds, i.e., an infinite gradient may not persist in a continuous solution when genuine nonlinearity holds.

4.1 Scalar conservation laws

A simplified alternative version of the previous section's proof is available in the case of a scalar conservation law:

$$u_t + c(u) u_x = 0 \tag{4.12}$$

where $c(u) = F'(u)$ with initial conditions

$$u(x, 0) = u_0(x). \tag{4.13}$$

Along characteristics

$$x = \chi(t; x_0) = x_0 + c(u_0(x_0))t \tag{4.14}$$

we have

$$u_x(x, t) = \frac{u_0'(x_0)}{1 + c'(u_0(x_0)) u_0'(x_0) t} = \frac{u_0'(x_0)}{1 + c'(u(x, t)) u_0'(x_0) t}, \tag{4.15}$$

(with prime indicating derivative with respect to the argument of u_0). If we consider a singularity where u_x is infinite along the characteristic $x = \chi(t; 0)$, say, then taking the limit $x \to \chi(t; 0)$ gives

$$u_x(x, t) \to \infty. \tag{4.16}$$

The corresponding limit for the initial condition implies that

$$u_0'(x_0) \to \infty \tag{4.17}$$

as $x_0 \to 0$, so that the blowup in the initial data is maintained:

$$u_x(x, t) = \frac{u_0'(x_0)}{1 + c'(u)u_0'(x_0)t} \to \infty\,. \tag{4.18}$$

However, the divergence of the numerator in the limit would be canceled by that in the denominator preventing a persistent infinite gradient in spatial derivative if it were not the case that $c'(u) = 0$, i.e., the failure of genuine nonlinearity in the scalar setting.

Remark 5. We note that the scalar case above can be realized in the multidimensional setting by restricting to simple waves (see Appendix).

5 Applications

For the remainder of the paper, we illustrate the theory of singular points developed above with three examples of quasilinear hyperbolic models of physical significance. Specifically, we first consider the Airy shallow water system

$$\begin{pmatrix} u_t \\ v_t \end{pmatrix} + \begin{pmatrix} u & 1 \\ v & u \end{pmatrix} \begin{pmatrix} u_x \\ v_x \end{pmatrix} = 0. \tag{5.1}$$

The second model is a two layer shallow water model in the Boussinesq limit (see e.g. [3]):

$$\begin{pmatrix} u_t \\ v_t \end{pmatrix} + \begin{pmatrix} (1-2u)v & u(1-u) \\ 1 - v^2 & (1-2u)v \end{pmatrix} \begin{pmatrix} u_x \\ v_x \end{pmatrix} = 0. \tag{5.2}$$

The third model we consider is the dispersionless modified Korteweg-de Vries equation, that is, the scalar law

$$u_t + u^2 u_x = 0 \tag{5.3}$$

which illustrates the key features of infinite gradients in simple wave solutions.

This section is organized as follows. We first recall some exact, self-similar solutions for system (5.1) which were used in [3, 2] to construct piecewise differentiable initial data for this system as well as to illustrate the non-splitting of corners in the evolution of this class of data. These solutions can also be used, under a non-invertible map, to construct solutions of system (5.2). Then, in section 5.2 a non-splitting corner in the Airy system is constructed. In section 5.3 an example from the two layer system, equation (5.2), exhibits non-splitting of a corner as well as the necessity of no critical points in the Riemann invariants for the conclusions of section 3 to hold. Then sections 5.4 and 5.5 demonstrate persistent infinite derivatives in simple wave solutions. Finally, section 5.6 contrasts the preceding cases by illustrating a persistent infinite gradient without a simple wave solution setup, which leads to a dynamically evolving angle with an adjacent slope.

5.1 Exact "core" solutions for Airy's system

For explicit examples we shall make use of the linear core solutions of the Airy system (5.1) from reference [1]:

$$u(x,t) = \alpha(t)x + \beta(t) \tag{5.4}$$

and

$$v(x,t) = \gamma(t)x + \delta(t) \tag{5.5}$$

where

$$\alpha(t) = \frac{\alpha_0}{1+\alpha_0 t}, \qquad \beta(t) = \frac{\beta_0 - \frac{\gamma_0}{\alpha_0}\log(1+\alpha_0 t)}{1+\alpha_0 t}, \tag{5.6}$$

$$\gamma(t) = \frac{\gamma_0}{(1+\alpha_0 t)^2}, \qquad \delta(t) = \frac{\delta_0}{1+\alpha_0 t} + \frac{\gamma_0(\frac{\gamma_0}{\alpha_0} - \beta_0)t}{(1+\alpha_0 t)^2} - \frac{\frac{\gamma_0^2}{\alpha_0^2}\log(1+\alpha_0 t)}{(1+\alpha_0 t)^2}. \tag{5.7}$$

The formulae for the characteristics $\chi_j(t;x_0)$ may be found by solving the equations

$$u(\chi_j(t;x_0),t) + 2(-1)^j\sqrt{v(\chi_j(t;x_0),t)} = R^{j0} = \alpha_0 x_0 + \beta_0 + 2(-1)^j\sqrt{\gamma_0 x_0 + \delta_0}, \tag{5.8}$$

which yields

$$\begin{aligned}\chi_j(t;x_0) = (1+\alpha_0 t)x_0 + t\left(\alpha_0 x_0 + \beta_0 + 2(-1)^j\sqrt{\gamma_0 x_0 + \delta_0}\right) \\ + \frac{2}{\alpha_0^2}\left(\gamma_0 + (-1)^j\alpha_0\sqrt{\gamma_0 x_0 + \delta_0}\right)(1 - \sqrt{1+\alpha_0 t}) + \frac{\gamma_0}{\alpha_0^2}\log(1+\alpha_0 t),\end{aligned} \tag{5.9}$$

with corresponding characteristic speeds

$$\lambda_j(u,v) = u + (-1)^j\sqrt{v}\,. \tag{5.10}$$

Such a solution may be spliced with a constant state via a simple wave (see [2]), i.e., the initial conditions are modified to be constant for $x > 0$ (or $x < 0$):

$$u_0(x) = \begin{cases} \beta_0 + \alpha_0 x, & x < 0 \\ \beta_0, & x \geq 0 \end{cases}, \qquad v_0(x) = \begin{cases} \delta_0 + \gamma_0 x, & x < 0 \\ \delta_0, & x \geq 0 \end{cases}. \tag{5.11}$$

In this way, examples may be constructed satisfying physical boundary conditions at $\pm\infty$ by placing the core between two constant states within the hyperbolic region. Since we are only concerned with the evolution of singularities with a definite position, we will only require that solutions under consideration are in the hyperbolic region in the part of the space-time half plane where these singularities occur. Because the Riemann invariants R^j are constant on the corresponding characteristics, the region of the $x-t$ plane, covered simultaneously by characteristics $x = \chi_j(t;x_0)$ for both $j = 1,2$ with $x_0 \leq 0$, will coincide with the linear core solution (u,v) in (5.4) and (5.5). Similarly, for the region of the $x-t$ plane covered by characteristics of both families emanating from the constant region, the solution will be constant. The right boundary curve of the left (linear core) region will be the characteristic of the first family emanating from $x_0 = 0$,

$$x = b_1(t) = t\left(\beta_0 - 2\sqrt{\delta_0}\right) + \frac{2}{\alpha_0^2}\left(\gamma_0 - \alpha_0\sqrt{\delta_0}\right)(1 - \sqrt{1+\alpha_0 t}) + \frac{\gamma_0}{\alpha_0^2}\log(1+\alpha_0 t) \equiv \chi_1(t;0)\,. \tag{5.12}$$

Further, the left boundary of the constant region will be the characteristic of the second family corresponding to $x_0 = 0$, which coincides with the one determined by the constant background state,

$$x = b_2(t) = \lambda_2(u_0(0), v_0(0))t = \lambda_2(\beta_0, \delta_0)t \equiv \chi_2(t;0). \tag{5.13}$$

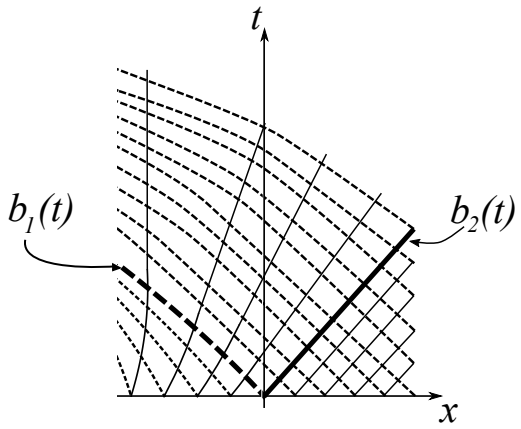

Figure 1: Sketch of the characteristic diagram with the linear core solution, the simple wave solution and the constant state. Dotted curves denote characteristics of the first family $j = 1$ and solid curves denote characteristics of the second family $j = 2$. The linear core solution's domain is to the left of the characteristic curve $x = b_1(t)$, for $x < b_1(t)$, and the constant background solution is to the right of characteristic line $x = b_2(t)$, for $x > b_2(t)$, with the simple wave solution's domain wedged in between, i.e., $b_1(t) \leq x \leq b_2(t)$.

The simple wave solution in the wedge middle region can then be constructed by enforcing the constancy of the Riemann invariants on characteristics,

$$R^1(x,t) = R^1(0,0) \tag{5.14}$$

for $b_1(t) < x < b_2(t)$, and

$$R^2\big(b_1(t_0) + (t-t_0)\lambda_2(b_1(t_0),t_0),t\big) = R^2(b_1(t_0),t_0). \tag{5.15}$$

Here, for convenience, we have written R^j and λ_j, $j = 1, 2$ in terms of their dependence on (x, t) directly rather than through their expressions in terms of (u, v). Then the identities

$$u = \frac{1}{2}(R^1 + R^2), \qquad v = \frac{1}{16}(R^1 - R^2)^2 \tag{5.16}$$

can be used to recover the solution in the simple wave region since R^1 is constant and $R^2(\chi_1(t_0;0),t_0)$ is given explicitly in terms of the linear core solution. We note that u and v are also constant on the characteristics $x = b_1(t_0) + (t - t_0)\lambda_2(b_1(t_0), t_0)$ since they are determined uniquely by the Riemann invariants (this holds even in the two layer case under the mapping (5.17), provided that a particular quadrant is chosen). A schematic of the characteristics in the $x - t$ plane is shown in figure 1.

In order to provide explicit solutions to system (5.2), we make use of a map [15, 4] relating it to system (5.1), allowing for the construction of explicit solutions with the type of singularities we have considered in the previous sections. This map is given by

$$\hat{u} = (1-2u)v, \qquad \hat{v} = (1-v^2)(u-u^2) \tag{5.17}$$

sending solutions (u, v) of system (5.2) to solutions $(u, v) = (\hat{u}, \hat{v})$ of system (5.1). The map (5.17) is many-to-one with $1 \to 4$ inverses (see [3]) given by

$$u_{ij} = \frac{1}{2}\left(1 + (\operatorname{sgn}\hat{u})^{j+1}(-1)^i\sqrt{Q - (-1)^j\sqrt{Q^2-\hat{u}^2}}\right) \tag{5.18}$$

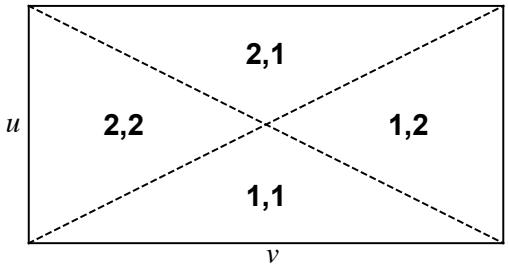

Figure 2: The i, j quadrant is the image of the curved triangle in figure 3 under (u_{ij}, v_{ij}) with v and u plotted on the horizontal and vertical axes respectively. The dotted lines are the singular curves of the map $(u, v) \to (\hat{u}, \hat{v})$.

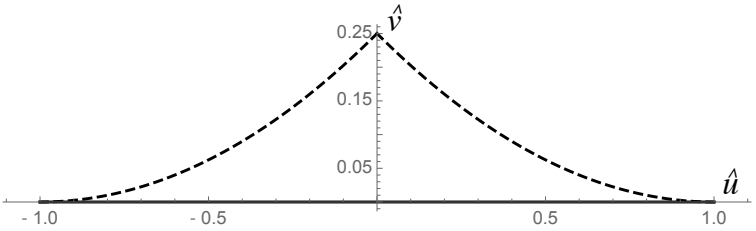

Figure 3: The image $\hat{\Omega}$ of the hyperbolic region Ω under the map $(u, v) \to (\hat{u}, \hat{v})$, with $\hat{u}$ and $\hat{v}$ plotted on the horizontal and vertical axes respectively. The dotted curves are the image of the singular curves (5.21).

and

$$v_{ij} = -(\operatorname{sgn} \hat{u})^j (-1)^i \sqrt{Q + (-1)^j \sqrt{Q^2 - \hat{u}^2}} \tag{5.19}$$

where $j = 1, 2$ and

$$Q = \frac{\hat{u}^2 - 4\hat{v} + 1}{2} \tag{5.20}$$

(here and afterwards we adorn the dependent variables with hats when they are obtained through the map (5.17), but not otherwise). Figure 2 shows the images of the four branches while figure 3 shows the image $\hat{\Omega}$ of the hyperbolic region Ω of the two layer system (5.2) under the map (5.17) along with the singular curves

$$u = \frac{1}{2} \pm \frac{v}{2}. \tag{5.21}$$

Note that these are level curves of the Riemann invariants

$$R^j(\hat{u}, \hat{v}) = \hat{u} + 2(-1)^j \sqrt{\hat{v}}\,, \tag{5.22}$$

with $j = 1, 2$, since

$$\begin{aligned} Q^2 - \hat{u}^2 &= \frac{1}{4}(1 - 2\hat{u}^2 + \hat{u}^4 - 8\hat{v} - 8\hat{u}^2\hat{v} + 16\hat{v}^2) \\ &= \frac{1}{4}((R^1)^2 - 1)((R^2)^2 - 1). \end{aligned} \tag{5.23}$$

5.2 Example 1: non-splitting corner in the Airy system

We use the linear core construction to present a solution which has a corner that does not split, corresponding to the lack of a jump in one of the Riemann invariants. We take initial conditions for which the linear core solutions (5.11) is set by

$$\alpha_0 = \gamma_0 = \delta_0 = 1\,, \qquad \text{and} \quad \beta_0 = 0\,. \tag{5.24}$$

Thus,

$$u_0(x) = \begin{cases} x, & x < 0 \\ 0, & x \geq 0 \end{cases}\,, \quad v_0(x) = \begin{cases} 1+x, & x < 0 \\ 1, & x \geq 0 \end{cases}\,. \tag{5.25}$$

The corresponding initial Riemann invariants are

$$R_0^j(x) = \begin{cases} x + 2(-1)^j\sqrt{1+x}, & x < 0 \\ 2(-1)^j, & x \geq 0 \end{cases}\,. \tag{5.26}$$

The derivative jumps of the Riemann invariants for the initial corner at $x_0 = 0$ are given by

$$[R_{0x}^j] = -1 - (-1)^j\,, \tag{5.27}$$

from which we may predict that the corner will not split given that only one of the Riemann invariants has a nonzero derivative jump. With the choice of initial conditions (5.24) the linear core solution is given by

$$u(x,t) = \frac{x - \log(1+t)}{1+t}\,, \qquad v(x,t) = \frac{x - \log(1+t) + 2t + 1}{(1+t)^2}, \tag{5.28}$$

and the leftmost characteristic (5.12) bounding the core solution is given by

$$x = b_1(t) = -2t + \log(1+t). \tag{5.29}$$

Having computed the basic elements explicitly, we turn to show that no corner will propagate along $x = b_1(t)$. To achieve this we must take the spatial derivatives on the right side, i.e., in the simple wave region where u and v are defined implicitly via the method of characteristics, and compare to the spatial derivatives defined by the linear core solution. The left derivatives are

$$u_x^l(b_1(t_0), t_0) = \alpha(t_0) = \frac{1}{1+t_0} \tag{5.30}$$

and

$$v_x^l(b_1(t_0), t_0) = \gamma(t_0) = \frac{1}{(1+t_0)^2}. \tag{5.31}$$

Then the right spatial derivative of u is

$$u_x^r(b_1(t_0), t_0) = \lim_{t \to t_0} \frac{u(x(t_0,t),t) - u(b_1(t),t)}{x(t_0,t) - b_1(t)} = \lim_{t \to t_0} \frac{u(b_1(t_0),t_0) - u(b_1(t),t)}{x(t_0,t) - b_1(t)}\,, \tag{5.32}$$

where $x(t_0,t) = b_1(t_0) + (t - t_0)\lambda_2(b_1(t_0), t_0)$, and

$$u_x^r = \frac{\dfrac{d}{dt_0}u(b_1(t_0),t_0)}{\dfrac{\partial x}{\partial t_0}(t_0,t_0)} = \frac{\dfrac{d}{dt_0}u(b_1(t_0),t_0)}{\lambda_1(b_1(t_0),t_0) - \lambda_2(b_1(t_0),t_0)}. \tag{5.33}$$

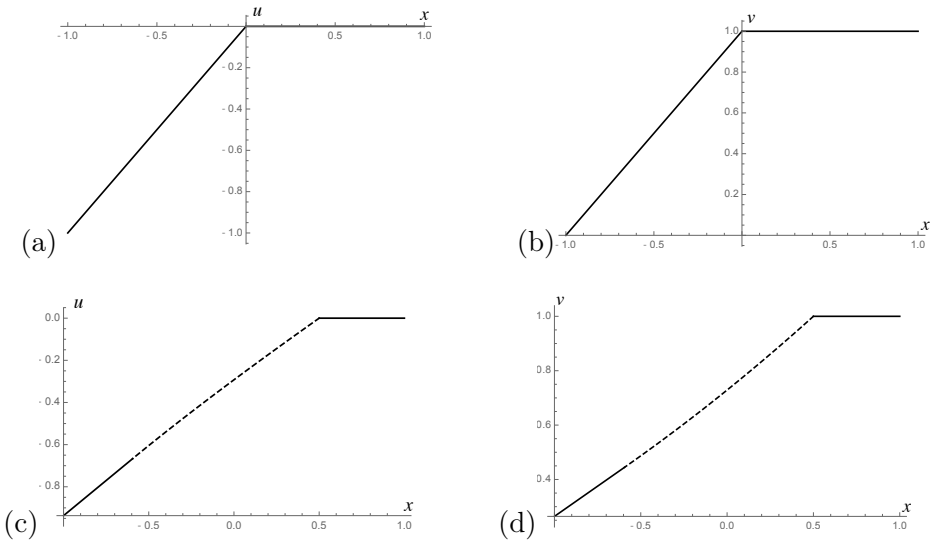

Figure 4: (a) and (b): Airy's system initial conditions (5.25), for which only one Riemann invariant has a corner; (c) and (d): the evolution of u and v, respectively, of these corner initial conditions at $t = 0.5$. The dash line is the simple wave that connects the background state to the linear core self-similar solution (5.28) with C^1 continuity at its splicing point, showing that no corner emerges there, while the corner persists between the simple wave and the constant background solution.

Identical manipulations yield

$$v_x^r = \frac{\dfrac{d}{dt_0} v(b_1(t_0), t_0)}{\lambda_1(b_1(t_0), t_0) - \lambda_2(b_1(t_0), t_0)}. \tag{5.34}$$

Thus we compute

$$\frac{d}{dt_0} u(b_1(t_0), t_0) = -\frac{2t_0}{(1+t_0)^2}, \qquad \frac{d}{dt_0} v(b_1(t_0), t_0) = -\frac{2t_0}{(1+t_0)^3}, \tag{5.35}$$

and

$$\lambda_1(b_1(t_0), t_0) - \lambda_2(b_1(t_0), t_0) = -\frac{2t_0}{1+t_0}. \tag{5.36}$$

Plugging these into the formulae (5.33) and (5.34) for the right (simple-wave-side) derivatives yields the same results as those for the left (linear-core-side) derivatives (5.30) and (5.31), so there is no jump along this characteristic. The initial condition in the top row of figure 4 evolves into the bottom row illustrating the non-splitting of the corner. In contrast, a generic case of both Riemann invariant possessing corners can simply be obtained by choosing a different initial slope $\alpha_0 \neq 1$. The case $\alpha_0 = 1.6$ yields the initial conditions and their evolution depicted in figure 5.

5.3 Example 2: non-splitting corner and singular Riemann invariant

In this section we consider a linear core solution[2] of the Airy system (5.1) which is tangent to the boundary of the domain of (u_{ij}, v_{ij}) and the images thereunder. That this property is maintained

[2]Since we are only concerned with local behavior at small time, we shall not, in this example, be concerned with splicing the linear core to a constant solution, with shock formation at large time, or with ellipticity away from points of interest.

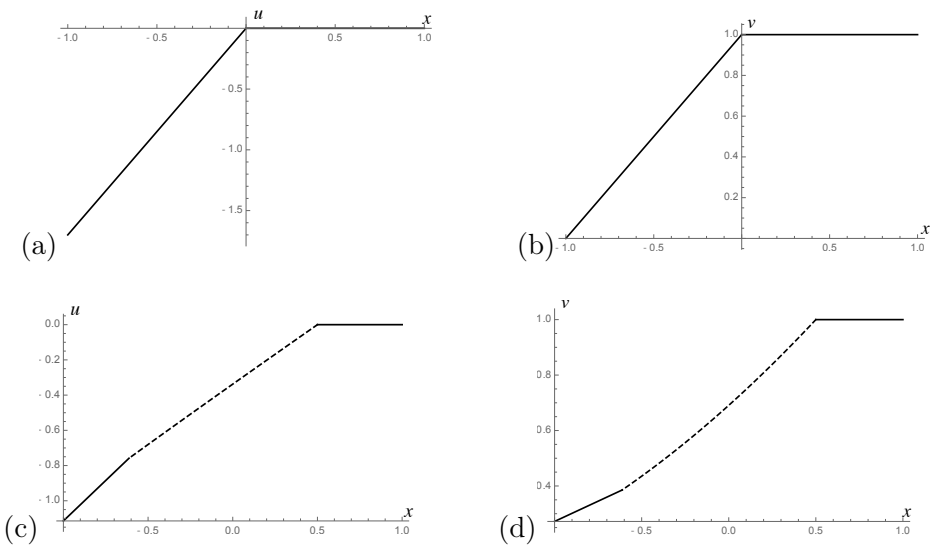

Figure 5: Same as figure 4 but with Airy's system initial conditions u_0 (a) and v_0 (b) for which both Riemann invariants have corners. Evolution of u (c) and v (d) at time $t = 0.5$: the splitting of corners at both ends of the simple wave connecting the linear core with the constant background can be clearly seen.

by evolution follows from the fact that this curve is a level surface of a Riemann invariant. An elementary computation shows that tangency can be achieved by setting

$$\beta_0 = \hat{u}_0, \qquad \gamma_0 = \frac{\alpha_0}{2}(\hat{u}_0 - 1), \qquad \delta_0 = \hat{v}_0 \tag{5.37}$$

where $(\hat{u}_0, \hat{v}_0) = (\hat{u}(0,0), \hat{v}(0,0))$ is the initial point of tangency and α_0 is a free parameter. For the present example we take $\beta_0 = 0.3$ and $\alpha_0 = 1$. The dependent variables in the $(\hat{u}, \hat{v})$ domain at time $t = 0$ and $t = 0.5$ are shown in figure 6.

Next, we consider the solutions to (5.2) in the $1, 1$ quadrant by mapping the linear core solution:

$$u(x,t) = u_{11}(\hat{u}(x,t), \hat{v}(x,t)), \qquad v(x,t) = v_{11}(\hat{u}(x,t), \hat{v}(x,t)), \tag{5.38}$$

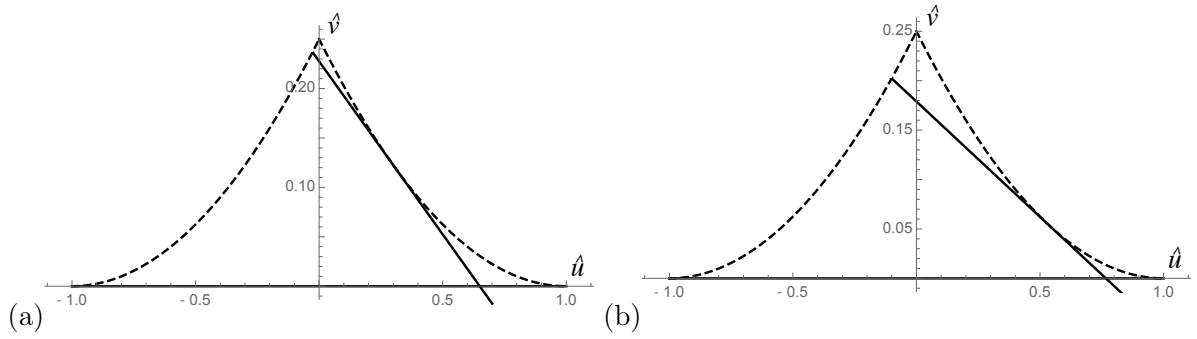

Figure 6: Linear core solutions tangent to the singular portion of the boundary of $\hat{\Omega}$ (see figure 3). Time $t = 0$ (a) and time $t = 0.5$ (b). The point of tangency slides to the right along critical curve during the evolution.

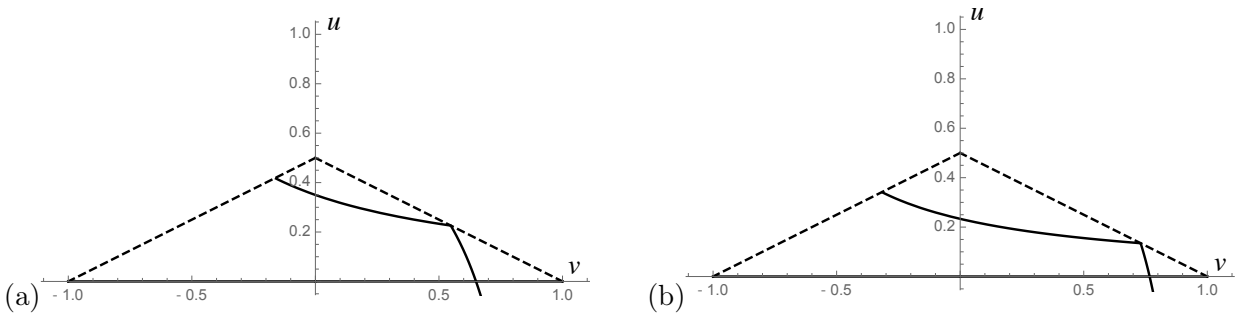

Figure 7: Pre-image of linear core solutions depicted in figure 6 in the $(1,1)$ quadrant, (a) at time $t = 0$ and (b) at time $t = 0.5$.

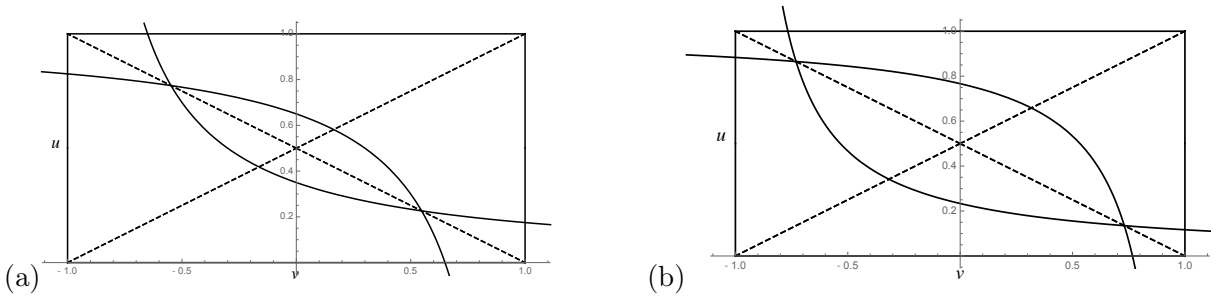

Figure 8: Total pre-image of linear core solutions in figure 6 in all quadrants, (a) at time $t = 0$ and (b) at time $t = 0.5$.

This solution is shown in the space of dependent variables at times $t = 0$ and $t = 0.5$ in figure 7 and the total pre-image of the linear core solution is shown in figure 8. The spatial dependence of u and v at fixed time are shown in figure 9.

We see that a single corner propagates in the solution (u, v), however the linear core solution is smooth by construction and the mapping from the system (5.1) to its Riemann invariants is also smooth in the hyperbolic region. Thus there are no corners in the initial Riemann invariants despite the fact that a single corner is achieved in the solution $(u(x,t), v(x,t))$. This is a consequence of the fact that the boundaries of the quadrants (i.e., the NGNL curves, see below), are each vanishing loci for the gradients of the corresponding Riemann invariants.

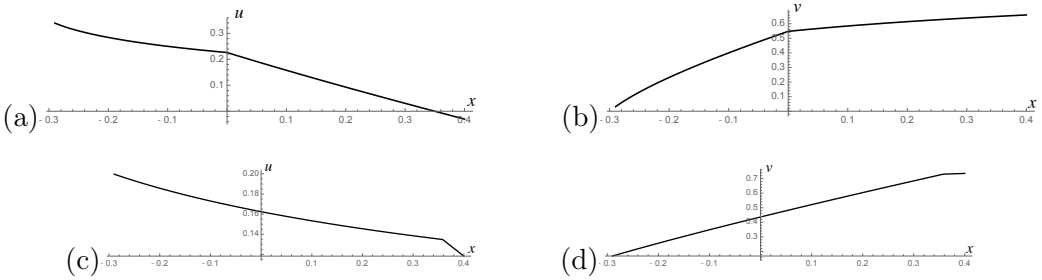

Figure 9: Snapshots of the solutions to system (5.2), which are depicted in the hodograph space by figure 7 at different times: initial condition (a) $u(x, 0)$ and (b) $v(x, 0)$; time evolution to $t = 0.5$ (c) $u(x, 0.5)$ and (d) $v(x, 0.5)$.

5.4 Example 3: Infinite gradient in a scalar conservation law

We provide an example of an infinite gradient which is not constant on either side, in the scalar case of section 4.1. Since simple waves are, by definition, solutions to a scalar law, the present example qualitatively illustrates the general situation where two simple waves of the same family are glued together at the NGNL point where the orientation of the curve reverses. This type of solution will eventually lead to shock formation at large enough time, but we may track the evolution prior to that while the infinite derivative is maintained, for a finite time interval, at a single point of a continuous solution profile.

We consider the simplest possible scalar law with the NGNL property: the cubic flux conservation law (5.3). With initial conditions $u(x,0) = u_0(x)$, the solution is given according to the method of characteristics:

$$u\big(x_0 + t\,u_0^2(x_0), t\big) = u_0(x_0). \tag{5.39}$$

With the choice of initial condition

$$u_0(x_0) = (\operatorname{sgn} x_0)\sqrt{|x_0|}, \tag{5.40}$$

we have

$$x = x_0(1 + (\operatorname{sgn} x_0)t) \tag{5.41}$$

which is single valued, having $\operatorname{sgn} x_0 = \operatorname{sgn} x$ when $t < 1$. Thus we may solve

$$x_0 = \frac{x}{1 + (\operatorname{sgn} x)t} \tag{5.42}$$

yielding

$$u(x,t) = (\operatorname{sgn} x)\sqrt{\frac{|x|}{1 + (\operatorname{sgn} x)t}}. \tag{5.43}$$

The evolution of the solution before shock time is shown in figure 10 (a,b). The same process may also be applied to the initial condition

$$u_0(x_0) = \sqrt{|x_0|}, \tag{5.44}$$

yielding the evolution

$$u(x,t) = \sqrt{\frac{|x|}{1 + (\operatorname{sgn} x)t}}. \tag{5.45}$$

shown in figure 10 (c,d).

5.5 Example 4: Infinite gradient in a centered simple wave

For the two layer system (5.2), the rarefaction curves (see Appendix for the setting) may be expressed explicitly. We take a centered simple wave solution in the $1,1$ quadrant:

$$u(x,t) = \begin{cases} u_l, & x/t \le \lambda_2(u_l, v_l) \\ u_{11}\left(-\frac{1}{3}(\frac{2x}{t} + \frac{1}{2}), \frac{1}{36}(\frac{2x}{t} - 1)\right), & \lambda_2(u_l, v_l) < x/t < \lambda_2(u_r, v_r) \\ u_r, & x/t \ge \lambda_2(u_r, v_r) \end{cases} \tag{5.46}$$

and

$$v(x,t) = \begin{cases} v_l, & x/t \le \lambda_2(u_l, v_l) \\ v_{11}\left(-\frac{1}{3}(\frac{2x}{t} + \frac{1}{2}), \frac{1}{36}(\frac{2x}{t} - 1)\right), & \lambda_2(u_l, v_l) < x/t < \lambda_2(u_r, v_r) \\ v_r, & x/t \ge \lambda_2(u_r, v_r) \end{cases} \tag{5.47}$$

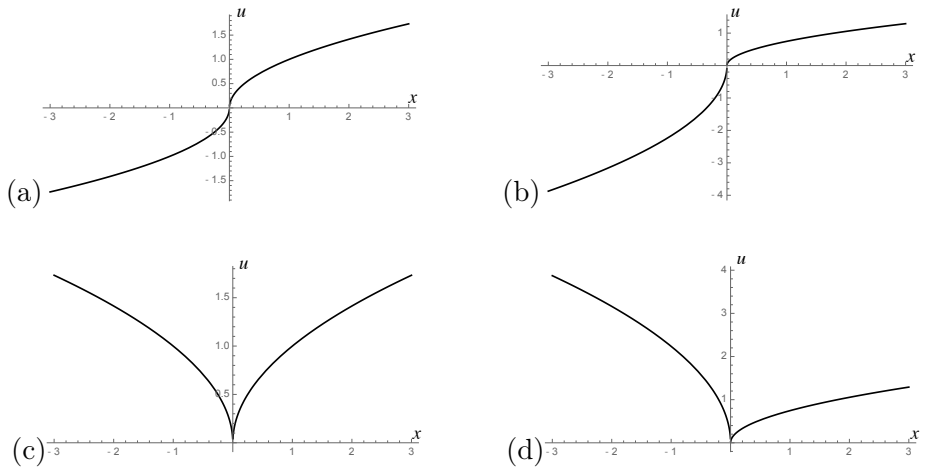

Figure 10: Snapshots of the evolution under the scalar law (5.3) of the two initial conditions (5.40) (top row), and (5.44) (bottom row). (a,c) time $t = 0$ and (b,d) time $t = 0.8$.

(with λ_2 defined in (5.10)), and we set

$$u_l = 0.15, \qquad v_l = 0.268466, \qquad u_r = 0.25, \qquad v_r = 0.5. \tag{5.48}$$

The initial conditions for this solution, approached in the limit $t \to 0^+$, are the step functions depicted in figure 11. As time evolves, as shown by the snapshots in this figure, the wave becomes less and less steep, except at the right state where the infinite gradient occurs. This is an NGNL point as can be seen in figure 12 where the simple-wave segment is shown in the hodograph space (u, v) of dependent variables.

5.6 Example 5: propagation of an infinite gradient spliced with a non-constant angle

In the previous infinite gradient examples the point in the space of dependent variables where an infinite gradient occurs remains constant in the evolution and, correspondingly, moves at a constant characteristic speed in the space-time half plane. This happens generically since the evolution along a characteristic for the hyperbolic system (2.1) occurs normally to the corresponding left eigenvector:

$$\boldsymbol{l}_k \cdot \frac{d}{dt}\boldsymbol{U}(\chi_k(t; x_0), t) = \boldsymbol{l}_k \cdot (\lambda_k I - D\boldsymbol{F}(\boldsymbol{U}))\boldsymbol{U}_x = 0, \tag{5.49}$$

whereas the NGNL manifold need not be normal to the left eigenvector. In the 2×2 case, non-constant evolution of the angle opposite the vertical tangent may occur on the NGNL curve only if the latter is a level set of a Riemann invariant. One particular instance where this is the case is the Boussinesq two layer system (5.2). We illustrate an explicit solution with an evolving infinite gradient point for this case. To accomplish this we consider the evolution obtained by connecting the linear core solution (5.11) with initial parameters

$$\alpha_0 = \frac{1}{3}, \qquad \beta_0 = -\frac{1}{3}, \qquad \gamma_0 = \frac{1}{3}, \qquad \delta_0 = \frac{1}{9} \tag{5.50}$$

on the left of the origin with the constant state $(\hat{u}, \hat{v}) = (\beta(t), \delta(t))$ on the right. Then a simple wave region will emerge between the rightmost characteristic $b_1(t)$ of the linear core and the leftmost

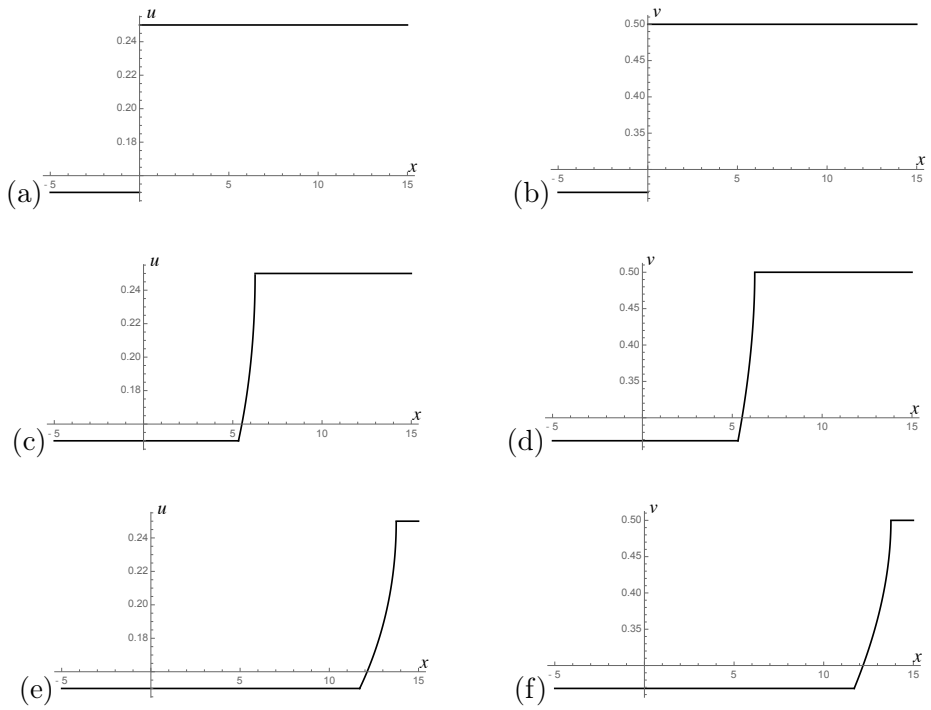

Figure 11: Initial conditions (a),(b) for the Riemann problem-like setup (5.46),(5.47): Snapshots of the evolution of the centered simple wave at time $t = 10$ (middle row) and time $t = 22$ bottom row. (c) $u(x, 10)$ (d) $v(x, 10)$; (e) $u(x, 22)$ (f) $v(x, 22)$.

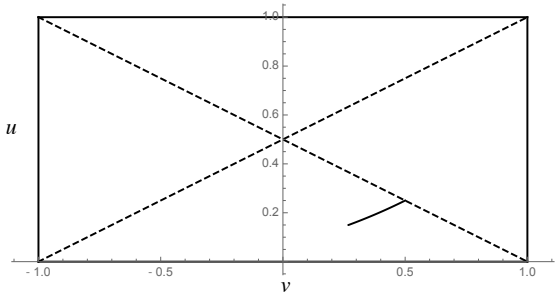

Figure 12: The simple wave segment (5.46),(5.47) shown in the hodograph (u, v)-plane.

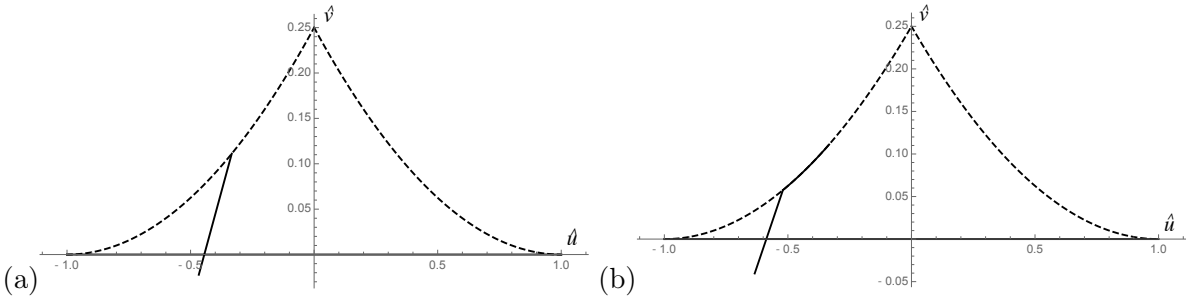

Figure 13: The solution in the $(\hat{u}, \hat{v})$ space (a) at time $t = 0$ and (b) at time $t = 0.5$.

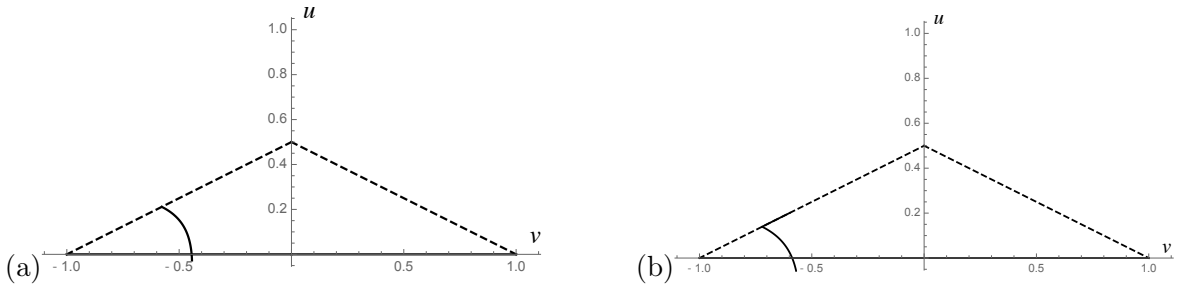

Figure 14: The solution to the two layer system, obtained from the $1,1$ branch of the mapping (5.17) applied to the solution in figure 13 (a) at time $t = 0$ and (b) at time $t = 0.5$.

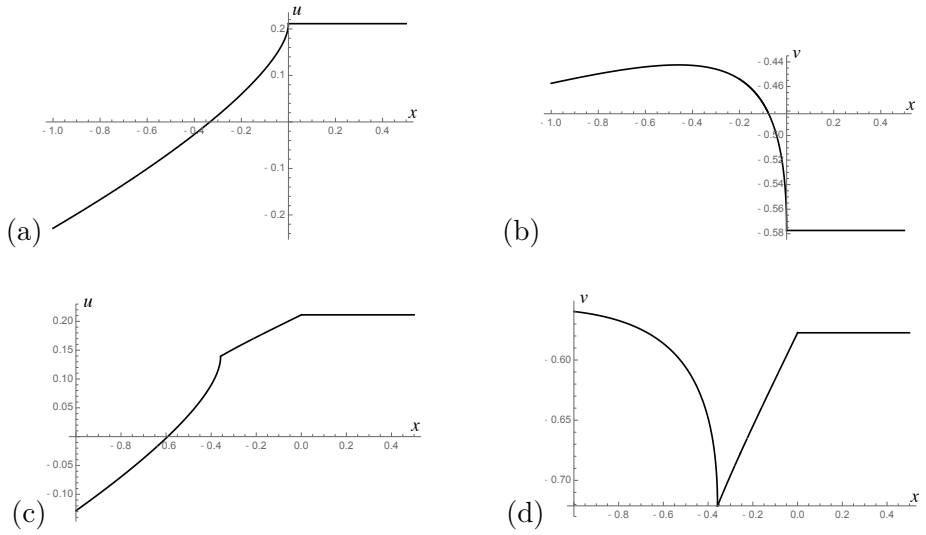

Figure 15: Snapshots of the solution from initial conditions obtained by the choice (5.50) and depicted in the $1,1$ quadrant in figure 14: initial condition (a) $u(x,0)$ and (b) and $v(x,0)$. Evolution of these initial conditions to time $t = 0.5$, (c) $u(x,0.5)$ and (d) $v(x,0.5)$.

characteristic $b_2(t)$ of the constant state. This simple wave coincides with the singular curve of the map (5.17) (see figure 13(b)). The infinite gradient propagates along $x = b_1(t)$, with dependent variables evolving along the NGNL curve, as shown in figure 15. We note that, unlike previous examples, the angle formed between the lines tangent to either component of the solution $u(x,\cdot)$, $v(x,\cdot)$ at the infinite gradient point is different from either $\pi/2$ (infinite gradient at the boundary of a constant state), π (front-like) or 0 (cusp), in contrast to our previous examples. This is apparent in figure 15 with the exact angle at a given time computable by the same method as in section 5.2.

6 Discussion and conclusions

We have described how initial discontinuities in derivatives evolve over time in hyperbolic systems, focusing on conditions by which an initial discontinuity can fission into multiple ones in the subsequent evolution. We have then considered the special case of a discontinuity occurring with an infinite derivative, and shown that such singularity may persist in a continuous solution without evolving in either a shock or relaxing to a finite corner if and only if genuine nonlinearity fails where the infinite derivative point lies in the hodograph plane.

The former development proves a conjecture from [3], about how corner splitting or fissioning by moving along characteristics can be obtained when their corresponding (multiple) Riemann invariants have initial derivative jumps. More precisely, splitting is obtained under this assumption except when (i) the corner point is also a critical point for the Riemann invariant, and (ii) quantities arising from differentiating the eigenvectors are not Lipschitz continuous. In both exceptional cases a corner in the initial Riemann invariant is sufficient for corner propagation. A counterexample to the necessity of condition (i) is provided in § 5.3: a corner which propagates along a characteristic despite the Riemann invariant of the corresponding family having no first derivative jump. Case (ii), on the other hand, is more pathological and further analysis would be required to fully address it.

Acknowledgments. This project was carried out with support by the National Science Foundation under grants RTG DMS-0943851, CMG ARC-1025523, DMS-1009750, DMS-1517879, DMS-1910824, DMS-2308063, by the Office of Naval Research under grants N00014-18-1-2490, N00014-23-1-2478 and DURIP N00014-12-1-0749, and by the European Union's Horizon 2020 research and innovation programme under the Marie Skłodowska-Curie grant no 778010 *IPaDEGAN*. We also gratefully acknowledge the auspices of the GNFM Section of INdAM, under which part of this work was carried out, and the financial support of the project MMNLP (Mathematical Methods in Non Linear Physics) of the INFN. RA, RC & MP thank the Department of Mathematics and its Applications of the University of Milano-Bicocca for its hospitality. RA & RC would also like to thank the Isaac Newton Institute for Mathematical Sciences, Cambridge, for support and hospitality during the programme HYD2 where work on this paper was completed, with support by EPSRC grant EP/R014604/1.

Appendix: Hyperbolic systems of conservation laws

In this appendix we briefly review some established results and constructions for hyperbolic systems of conservation laws in a single space dimension. Given that discontinuities often form at some finite time for solutions of (2.2) even with continuously differentiable initial data, it is natural to consider initial conditions that are already discontinuous. Reference [8] in fact uses an iterative approximation of initial conditions by step functions to prove existence of solutions with initial data having small total variation. The hyperbolic system (2.1) (or more precisely (2.2)) is solved in reference [9] for initial data $\boldsymbol{U}_0$ as the simple step function

$$\boldsymbol{U}_0(x) = \begin{cases} \boldsymbol{U}^l, & x < 0 \\ \boldsymbol{U}^r, & x > 0 \end{cases} \tag{A1}$$

with the distance between $\boldsymbol{U}^l$ and $\boldsymbol{U}^r$ sufficiently small, under the assumption (2.6) of genuine nonlinearity. The building blocks of the solution are k-waves: curves $\boldsymbol{W}_k(\xi_k; \boldsymbol{U}^l)$ in the space of dependent variables which, for $\xi_k \geq \lambda_k(\boldsymbol{U}^l)$, are integral curves of $\boldsymbol{r}_k$, where the scaling of the $\boldsymbol{r}_k$ is chosen such that

$$D\lambda_k(\boldsymbol{U}) \cdot \boldsymbol{r}_k = 1. \tag{A2}$$

Thus we have that

$$\frac{d}{d\xi_k} \boldsymbol{W}_k(\xi_k; \boldsymbol{U}^l) = \boldsymbol{r}_k(\boldsymbol{W}_k(\xi_k; \boldsymbol{U}^l)), \tag{A3}$$

with $\xi_k = \lambda_k(\boldsymbol{W}_k(\xi_k; \boldsymbol{U}^l))$. For $\xi_k < \lambda_k(\boldsymbol{U}^l)$ these curves are defined implicitly by the constraints

$$\boldsymbol{F}(\boldsymbol{W}_k(\xi_k; \boldsymbol{U}^l)) - \boldsymbol{F}(\boldsymbol{U}^l) = \sigma_k(\xi_k)(\boldsymbol{W}_k(\xi_k; \boldsymbol{U}^l) - \boldsymbol{U}^l), \tag{A4}$$

known as the Rankine-Hugoniot conditions, with

$$\sigma_k(\lambda_k(\boldsymbol{U}^l)) = \lambda_k(\boldsymbol{U}^l). \tag{A5}$$

Genuine nonlinearity (equation (2.6)) ensures, among other things, that $\boldsymbol{W}_k(\xi_k; \boldsymbol{U}^l)$ for $\xi_k > \lambda_k(\boldsymbol{U}^l)$ is well defined. In [9] the condition

$$\lambda_k(\boldsymbol{W}_k(\xi_k; \boldsymbol{U}^l)) < \sigma_k(\xi_k) < \lambda_k(\boldsymbol{U}^l) \tag{A6}$$

for $\xi_k < \lambda_k(\boldsymbol{U}^l)$, is formulated, which ensures that the $\xi_k < \lambda_k(\boldsymbol{U}^l)$ construction is unique (and physically relevant). It can be shown that $\boldsymbol{W}_k$ is then twice continuously differentiable in ξ_k, even at $\xi_k = \lambda_k(\boldsymbol{U}^l)$. A solution to the hyperbolic system (2.2) with initial data (A1) having $\boldsymbol{U}^r = \boldsymbol{W}_k(\xi_k; \boldsymbol{U}^l)$ is furnished, for $\xi_k > \lambda_k(\boldsymbol{U}^l)$:

$$\boldsymbol{U}(x,t) = \begin{cases} \boldsymbol{U}^l, & x/t \le \lambda_k(\boldsymbol{U}^l) \\ \boldsymbol{W}_k(x/t; \boldsymbol{U}^l), & \lambda_k(\boldsymbol{U}^l) < x/t < \lambda_k(\boldsymbol{U}^r) \\ \boldsymbol{U}^r, & x/t \ge \lambda_k(\boldsymbol{U}^r) \end{cases} \tag{A7}$$

or for $\xi_k < \lambda_k(\boldsymbol{U}^l)$, discontinuous solutions to (2.2), called shocks, can be constructed:

$$\boldsymbol{U}(x,t) = \begin{cases} \boldsymbol{U}^l, & x/t < \sigma_k(\xi_k) \\ \boldsymbol{U}^r, & x/t > \sigma_k(\xi_k) \end{cases}. \tag{A8}$$

It can be checked that equation (A4) ensures that $\boldsymbol{U}$ solves system (2.2). A unique solution to (2.2)-(A1) can then be constructed for any $\boldsymbol{U}^r$ that can be reached by gluing together consecutive $\boldsymbol{W}_k$ curves, $k = 1, 2, 3, ..., n$:

$$\boldsymbol{U}^r = \boldsymbol{W}_k(\xi_k; \boldsymbol{W}_{k-1}(\xi_{k-1}; (...(\boldsymbol{W}_1(\xi_1; \boldsymbol{U}^l))...))) \tag{A9}$$

provided that

$$\lambda_{k-1}(\boldsymbol{U}^r_{k-1}) < \sigma_k(\xi_k) < \lambda_{k+1}(\boldsymbol{U}^r_k) \tag{A10}$$

where

$$\boldsymbol{U}^r_j = \boldsymbol{W}_j(\xi_j; \boldsymbol{U}^r_{j-1}) \quad \text{and} \quad \boldsymbol{U}^r_0 = \boldsymbol{U}^l \tag{A11}$$

whenever $\xi_k < 0$. Equations (A10) and (A6) are known as the Lax Entropy Conditions. The set of $\boldsymbol{U}^r$ reachable in this fashion is shown in [9] to have $\boldsymbol{U}^l$ as an interior point and the solution is unique for a sufficiently small neighborhood of $\boldsymbol{U}^l$.

A centered simple wave solution $\boldsymbol{W}_k(\xi_k(\zeta); \boldsymbol{U}^l)$, with genuine nonlinearity failing for the k-th family, has an infinite gradient. In fact, we may parametrize the simple wave curve by ζ for which the tangent

$$\frac{d}{d\zeta}\boldsymbol{W}_k(\xi_k(\zeta); \boldsymbol{U}^l) = \tilde{\boldsymbol{r}}_k \tag{A12}$$

has unit length, $|\tilde{\boldsymbol{r}}_k|^2 = 1$. Then the centered simple wave solution (A7) has spatial derivative

$$\begin{aligned} \frac{d}{dx}\boldsymbol{W}_k(x/t; \boldsymbol{U}^l) &= \frac{d\xi_k}{dx}\frac{d\zeta}{d\xi}\frac{d}{d\zeta}\boldsymbol{W}_k \\ &= \frac{d\xi_k}{dx}\frac{d\zeta}{d\xi}\tilde{\boldsymbol{r}}_k \\ &= \frac{d\xi_k}{dx}\frac{1}{D\lambda_k(\tilde{\boldsymbol{r}}_k)}\tilde{\boldsymbol{r}}_k \end{aligned} \tag{A13}$$

and since $D\lambda_k(\tilde{\boldsymbol{r}}_k) \to 0$ as $x/t \to \lambda_k(\boldsymbol{U}^l)$, the spatial derivative blows up, $\frac{d}{dx}\boldsymbol{W}_k(x/t; \boldsymbol{U}^l) \to \pm\infty$.

References

[1] R. Camassa, G. Falqui, G. Ortenzi, M. Pedroni, On the geometry of extended self-similar solutions of the Airy shallow water equations. *SIGMA*, **15** (2019), 17 pages.

[2] R. Camassa, G. Falqui, G. Ortenzi, M. Pedroni, G. Pitton, On the "vacuum" dam-break problem: Exact solutions and their long time asymptotics. *SIAM J. Appl. Math.*, **80** (2020), 44–70.

[3] R. Camassa, G. Falqui, G. Ortenzi, M. Pedroni, C. Thomson, Hydrodynamic models and confinement effects by horizontal boundaries. *J. Nonl. Sci.*, **29** (2019), 1445–1498.

[4] L. Chumakova, F.E. Menzaque, P.A. Milewski, R.R. Rosales, E.G. Tabak, C.V. Turner, Stability properties and nonlinear mappings of two and three-layer stratified flows. *Studies Appl. Math.*, **122** (2009), 123–137.

[5] C.M. Edwards, S.D. Howison, H. Ockendon, J.R. Ockendon, Non-classical shallow water flows. *IMA J. Appl. Math.*, **73** (2007), 137–157.

[6] G.A. El, M.A. Hoefer, M. Shearer, Dispersive and diffusive-dispersive shock waves for nonconvex conservation laws. *SIAM Review*, **59** (2017), 3–61.

[7] I.M. Gelfand & G.E. Shilov, *Generalized Functions.* Academic Press, New York, 1964.

[8] J. Glimm, *Solutions in the large for nonlinear hyperbolic systems of equations. Comm. Pure Appl. Math.*, **18** (1965), 697–715.

[9] P.D. Lax, *Hyperbolic systems of conservation laws. Comm. Pure Appl. Math.*, **10** (1957), 537–566.

[10] P. D. Lax, *The initial value problem for nonlinear hyperbolic equations in two independent variables,* in Contributions to the Theory of Partial Differential Equations, *Ann. of Math. Stud. 33*, Princeton University Press, Princeton, NJ, 1954, pp. 211-229.

[11] P.G. LeFloch, *Hyperbolic Systems of Conservation Laws: The Theory of Classical and Nonclassical Shock Waves. Lectures in Mathematics ETH Zürich*, Birkhäuser, Basel, 2002.

[12] P.G. LeFloch, M.D. Thanh, Nonclassical Riemann solvers and kinetic relations I. A nonconvex hyperbolic model of phase transitions. *ZAMP*, **52** (2001), 597–619.

[13] T.P. Liu, The Riemann problem for general 2×2 conservation laws. *Trans. Amer. Math. Soc.*, **199** (1974), 89–112.

[14] T.P. Liu, The Riemann problem for general systems of conservation laws. *J. Diff. Eq.*, **18** (1975), 218–234.

[15] L.V. Ovsyannikov, Two-layer "shallow water" model. *Journal of Applied Mechanics and Technical Physics*, **20** (1979), 127–135.

[16] M.R. Schulze, M. Shearer, Undercompressive shocks for a system of hyperbolic conservation laws with cubic nonlinearity. *J. Math. Anal. Appl.*, **229** (1999), 334–362.

[17] G.B. Whitham, *Linear and Nonlinear Waves.* John Wiley & Sons, New York, 1999.